the denc

Department:
Environment & Nature Conservation
NORTHERN CAPE PROVINCE
REPUBLIC OF SOUTH AFRICA

# Strategy Development

environmental affairs
Department:
Environmental Affairs
REPUBLIC OF SOUTH AFRICA

giz Deutsche Gesellschaft für Internationale Zusammenarbeit (GIZ) GmbH

PM ENVIROTECH SOLUTIONS

**Table of Contents**

# 1. Introduction

Climate change is projected to impact drastically in southern African during the 21st century under low mitigation futures (Niang et al., 2014). African temperatures are projected to rise rapidly, in the subtropics at least at 1.5 times the global rate of temperature increase (James and Washington, 2013; Engelbrecht et al., 2015). Moreover, the southern African region is projected to become generally drier under enhanced anthropogenic forcing (Christensen et al., 2007; Engelbrecht et al., 2009; James and Washington, 2013; Niang et al., 2014). These changes in temperature and rainfall patterns will plausibly have a range of impacts in South Africa, including impacts on energy demand (in terms of achieving human comfort within buildings and factories), agriculture (e.g. reductions of yield in the maize crop under higher temperatures and reduced soil moisture), livestock production (e.g. higher cattle mortality as a result of oppressive temperatures) and water security (through reduced rainfall and enhanced evapotranspiration) (Engelbrecht et al., 2015).

It is important to realise that climate change is not to take place only through changes in average temperature and rainfall patterns, but also through changes in the attributes of extreme weather events. For the southern African region, generally drier conditions and the more frequent occurrence of dry spells are plausible (Christensen et al., 2007; Engelbrecht et al., 2009). Tropical cyclone tracks are projected to shift northward, bringing more flood events to northern Mozambique and fewer to the Limpopo province in South Africa (Malherbe et al., 2013). Cut-off low related flood events are also projected to occur less frequently over South Africa (e.g. Engelbrecht et al., 2013) in response to a poleward displacement of the westerly wind regime. Intense thunderstorms are plausible to occur more frequently over South Africa in a generally warmer climate (e.g. Engelbrecht et al., 2013).

The purpose of this report is to provide an update on the latest insights and evidence available regarding future changes in climatological averages and extreme events over South Africa, with a focus on changes that are to impact on the Northern Cape Province. Recent downscalings of global circulation model (GCM) projections of the Coupled Model Inter-comparison Project Phase Five (CMIP5) and Assessment Report Five (AR5) of the Intergovernmental Panel on Climate Change (IPCC), obtained at the Council for Scientific and Industrial Research (CSIR) and the Commonwealth Scientific and Industrial Research Organisation (CSIRO), are used for this purpose. These downscalings are for the period 1971 to 2100, follow the experimental design recommended by the Coordinated Downscaling Experiment (CORDEX) and have been derived for both low and high mitigation scenarios. The regional climate model used to obtain the downscalings is the conformal-cubic atmospheric model (CCAM) of the CSIRO. In addition, the report also considers evidence on changes in extreme events over Southern Africa as presented in Assessment Report Four (AR4) and AR5 of the IPCC (Christensen et al., 2007; Niang et al., 2014) and in the Long Term Adaptation Scenarios Report (LTAS, 2013) of the Department of Environmental Affairs (DEA).

# 2. Experimental design and model verification

Regional climate modelling is used to downscale the projections of CMIP5 GCMs to high resolution over southern Africa. The regional climate model used, CCAM, is a variable-resolution GCM developed by the CSIRO (McGregor 2005; McGregor and Dix 2001, 2008). The model solves the hydrostatic primitive equations using a semi-implicit semi-Lagrangian solution procedure, and includes a comprehensive set of physical parameterizations. The GFDL parameterization for long-wave and shortwave radiation (Schwarzkopf and Fels 1991) is employed, with interactive cloud distributions determined by the liquid and ice-water scheme of Rotstayn (1997). The model employs a stability-dependent boundary layer scheme based on Monin-Obukhov similarity theory (McGregor et al. 1993). CCAM runs coupled to a dynamic land-surface model CABLE (CSIRO Atmosphere Biosphere Land Exchange model). The cumulus convection scheme uses mass-flux closure, as described by McGregor (2003), and includes both downdrafts and detrainment. CCAM may be employed in quasi-uniform mode or in stretched mode by utilising the Schmidt (1977) transformation.

Six GCM simulations of CMIP5 and AR5 of the IPCC, obtained for the emission scenarios described by Representative Concentration Pathways 4.5 and 8.5 (RCP4.5 and 8.5) were downscaled to 50 km resolution globally. The simulations span the period 1971-2100. RCP4.5 is a high mitigation scenario, whilst RCP8.5 is a low mitigation scenario. The GCMs downscaled are the Australian Community Climate and Earth System Simulator (ACCESS1-0); the Geophysical Fluid Dynamics Laboratory Coupled Model (GFDL-CM3); the National Centre for Meteorological Research Coupled Global Climate Model, version 5 (CNRM-CM5); the Max Planck Institute Coupled Earth System Model (MPI-ESM-LR) and the Model for Interdisciplinary Research on Climate (MIROC4h). The simulations were performed on supercomputers of the CSIRO (Katzfey et al., 2012) and on the Centre for High Performance Computing (CHPC) of the Meraka Institute of the CSIR in South Africa.

In these simulations CCAM was forced with the bias-corrected daily sea-surface temperatures (SSTs) and sea-ice concentrations of each host model, and with $CO_2$, sulphate and ozone forcing consistent with the RCP4.5 and 8.5 scenarios. The model's ability to realistically simulate present-day Southern African climate has been extensively demonstrated (e.g. Engelbrecht et al., 2009; Engelbrecht et al., 2011; Engelbrecht et al., 2013; Malherbe et al., 2013; Winsemius et al., 2014; Engelbrecht et al., 2015). Most current coupled GCMs do not employ flux corrections between atmosphere and ocean, which contributes to the existence of biases in their simulations of present-day SSTs – more than 2 $^{o}$C along the West African coast. The bias is computed by subtracting for each month the Reynolds (1988) SST climatology (for 1961-2000) from the corresponding GCM climatology. The bias-correction is applied consistently throughout the simulation. Through this procedure the climatology of the SSTs applied as lower boundary forcing is the same as that of the Reynolds SSTs. However, the intra-annual variability and climate-change signal of the GCM SSTs are preserved (Katzfey et al., 2009).

### 2.1. Model projections of the changing patterns of climate and extreme weather events over South Africa under enhanced anthropogenic forcing

In this section the projected changes in a number of climatological variables (Table 1), including extreme weather-events metrics, are presented. For each of the metrics under consideration, the simulated baseline (climatological) state over South Africa calculated for the period 1971-2000 is shown in a first Figure (note that the median of the six downscalings is shown in this case). The projected changes in the metric are subsequently shown, for the time-slab 2020-2050 relative to the baseline period 1971-2000, first for RCP8.5 (low mitigation) and then for RCP4.5 (high mitigation). Three figures are presented for each metric for each RCP, namely the 10th, 50th (median) and 90th percentiles of the ensemble of projected changes under the RCP. In this way, it is possible to gain some understanding of the uncertainty range that is associated with the projections.

**Table 2.1:** Relevant climate variables projected by the ensemble models under RCP4.5 and RCP 8.5 mitigation scenarios for the periods 1921 – 2000 and 2020- 2050

| Variable | Description and/or units |
|---|---|
| **Average temperature** | °C |
| **Very hot days** | A day when the maximum temperature exceeds 35 °C. Units are number of events per grid point per year. |
| **Heat-wave days** | The maximum temperature exceeds the average temperature of the warmest month of the year by 5 °C for at least 3 days. |
| **High fire-danger days** | McArthur fire-danger index exceeds a value of 24. Units are number of events per grid point per year. |
| **Rainfall** | Mm |
| **Extreme rainfall Type I event (also a proxy for lightning)** | More than 20 mm of rain falling within 24 hrs over an area of 50 x 50 $km^2$. The occurrence of extreme convective rainfall is used as a proxy for the occurrence of storms that produce lightning. Units are number of events per grid point per year. |
| **Dry-spell** | Five or more consecutive days without rainfall (units are number of days per grid point per year) |

# 3. Projected climate futures for the Northern Cape Province

## 3.1 Average Temperatures

For the present-day conditions (1971-2000) the model simulations are indicative of highest temperatures occurring over the northern parts of the Northern Cape Province (Figure 3.1 a).

- For the near future (2020-2050), the projections are indicative of increases in temperature of between 1 and 3°C under low mitigation. The north eastern part of the province is expected to warm most with 3° C temperature increases being plausible (Figure 3.2 b (a-f)).
- Under the RCP 4.5 (high mitigation scenario) an increase in temperature of between 1-2° C is plausible across the province, with some downscalings indicating temperature increases as high as 2.5 °C over the northern parts of the province.
- Rising temperatures are plausible to be associated with a decrease in the household demand for energy (warming) in winter and an increase in energy demand for cooling in summer.

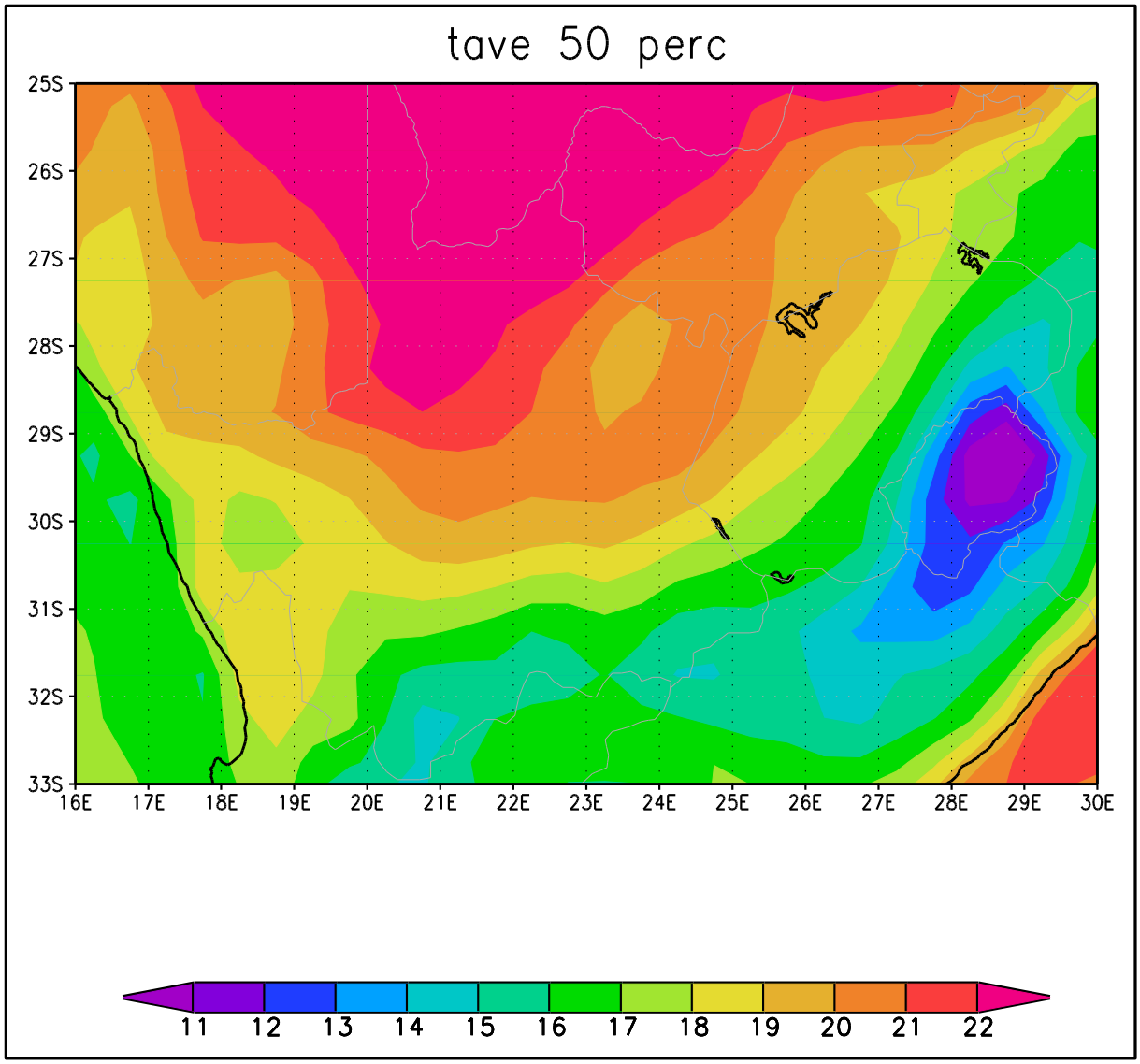


Figure 3.1 a: CCAM simulated annual average temperature (°C) over the Northern Cape for the baseline period 1971-2000. The median of simulations is shown for the ensemble of downscalings of six GCM simulations.

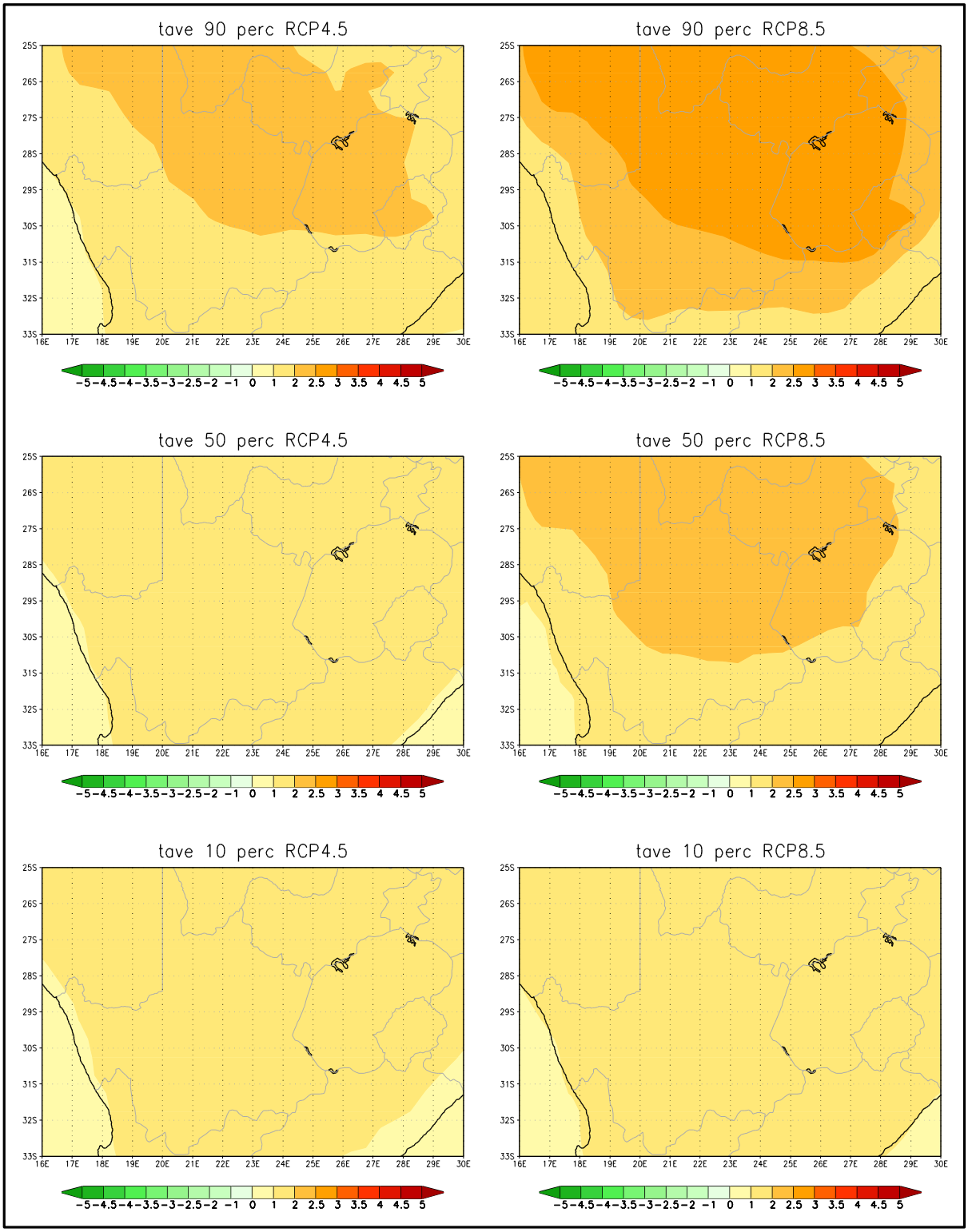
tave 90 perc RCP4.5
tave 90 perc RCP8.5
tave 50 perc RCP4.5
tave 50 perc RCP8.5
tave 10 perc RCP4.5
tave 10 perc RCP8.5
25S 26S 27S 28S 29S 30S 31S 32S 33S
16E 17E 18E 19E 20E 21E 22E 23E 24E 25E 26E 27E 28E 29E 30E
-5 -4.5 -4 -3.5 -3 -2.5 -2 -1 0 1 2 2.5 3 3.5 4 4.5 5

Figure 3.1 b (a-f): CCAM projected change in the annual average temperature (°C) over the Northern Cape for the time-slab 2020-2050 relative to 1971-2000. The 10th, 50th and 90th percentiles are shown for the ensemble of downscalings of six GCM projections under RCP4.5 (left) and RCP8.5 (right).

### 3.2.2 Very hot days

- In association with a drastic increase in temperatures the number of very hot days in the Northern Cape is also projected to increase drastically.
- Under the low mitigation scenario increases in the number of hot days of between 30-60 days per annum are projected; with the highest increases projected for the northern parts of the province.
- For the high mitigation scenario the number of very hot days is still projected to increase significantly, with 20-50 more of these days projected to occur annually (Figure 3.2 b (a-f)).

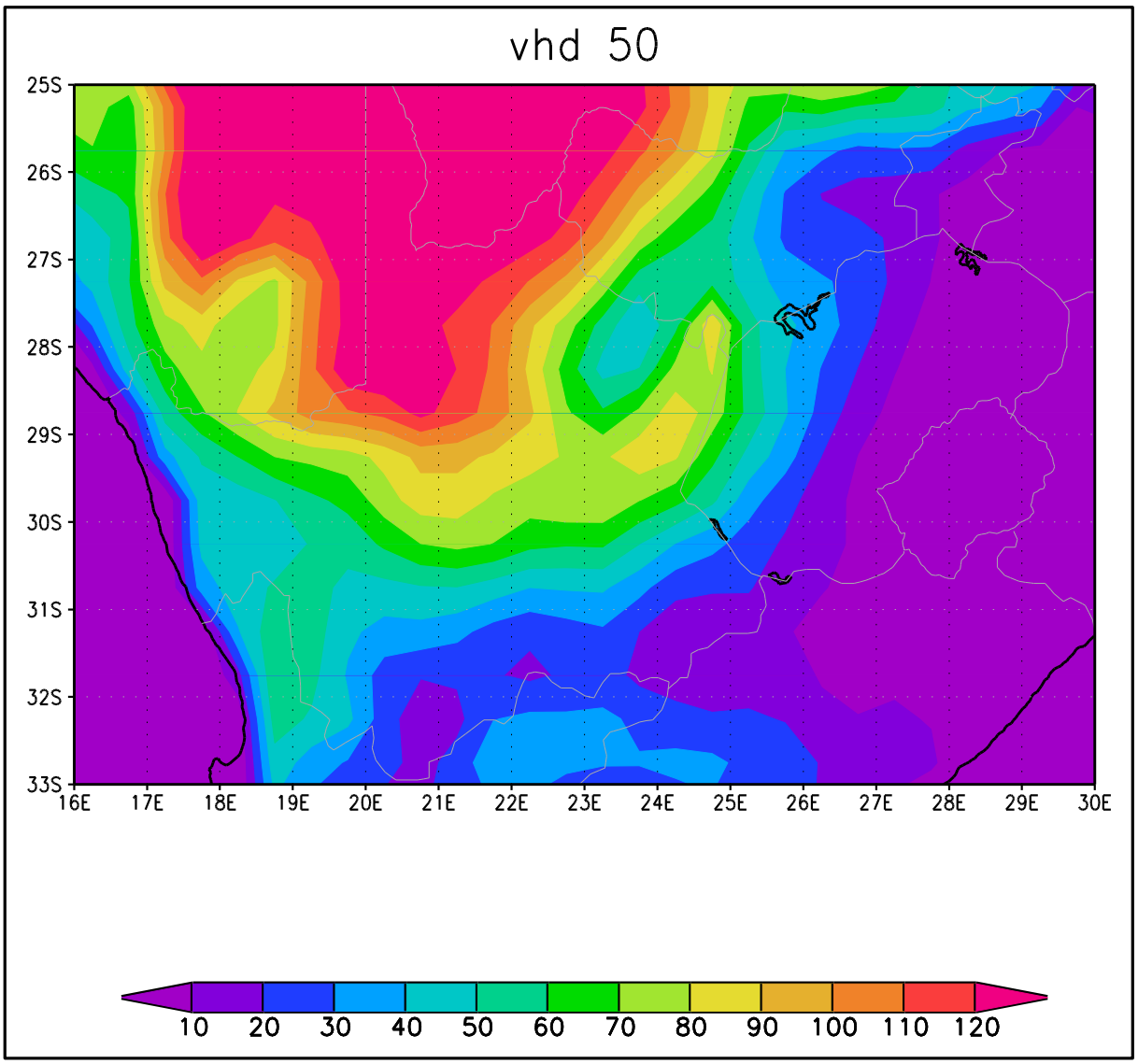


Figure 3.2 a: CCAM simulated annual average number of very hot days (units are number of days per grid point per year) over the Northern Cape for the baseline period 1971-2000. The median of simulations is shown for the ensemble of downscalings of six GCM simulations.

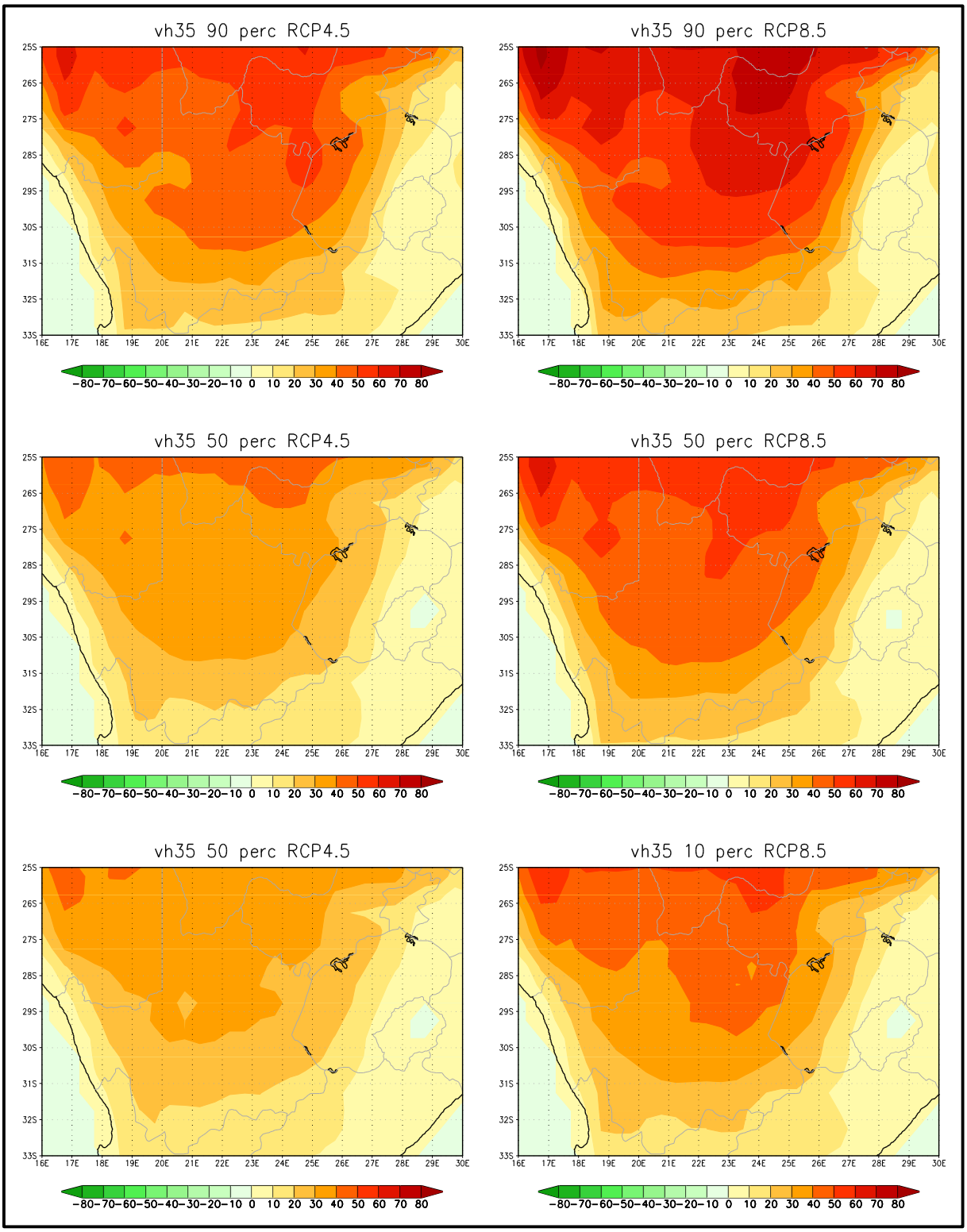
vh35 90 perc RCP4.5
vh35 90 perc RCP8.5
vh35 50 perc RCP4.5
vh35 50 perc RCP8.5
vh35 50 perc RCP4.5
vh35 10 perc RCP8.5
25S 26S 27S 28S 29S 30S 31S 32S 33S
16E 17E 18E 19E 20E 21E 22E 23E 24E 25E 26E 27E 28E 29E 30E
-80 -70 -60 -50 -40 -30 -20 -10 0 10 20 30 40 50 60 70 80

Figure 3.2 b (a-f): CCAM projected change in the annual average number of very hot days (units are days per grid point per year) over the Northern Cape for the time-slab 2021-2050 relative to 1971-2000. The 10$^{th}$, 50th and 90th percentiles are shown for the ensemble of downscalings of six GCM projections under RCP4.5 (left) and RCP8.5 (right).

### 3.2.3 Heat -wave days

Less than 10 heat-wave days are simulated to occur annually on the average, within the present-day climate of the Northern Cape.

- Under high mitigation the number of heat-wave days is projected to increase by about 10 events per year (Figure 3.3 a). The largest increases are projected for the northern parts of the province.
- Under the low mitigation scenario the number of heat wave days may increase by as many as 20 events per year (Figure 3.3 b (a-f)). Such a drastic increase in the number of heat wave days may have impacts on the health of people and animals in the province, through the increased occurrence of these oppressive temperature events.

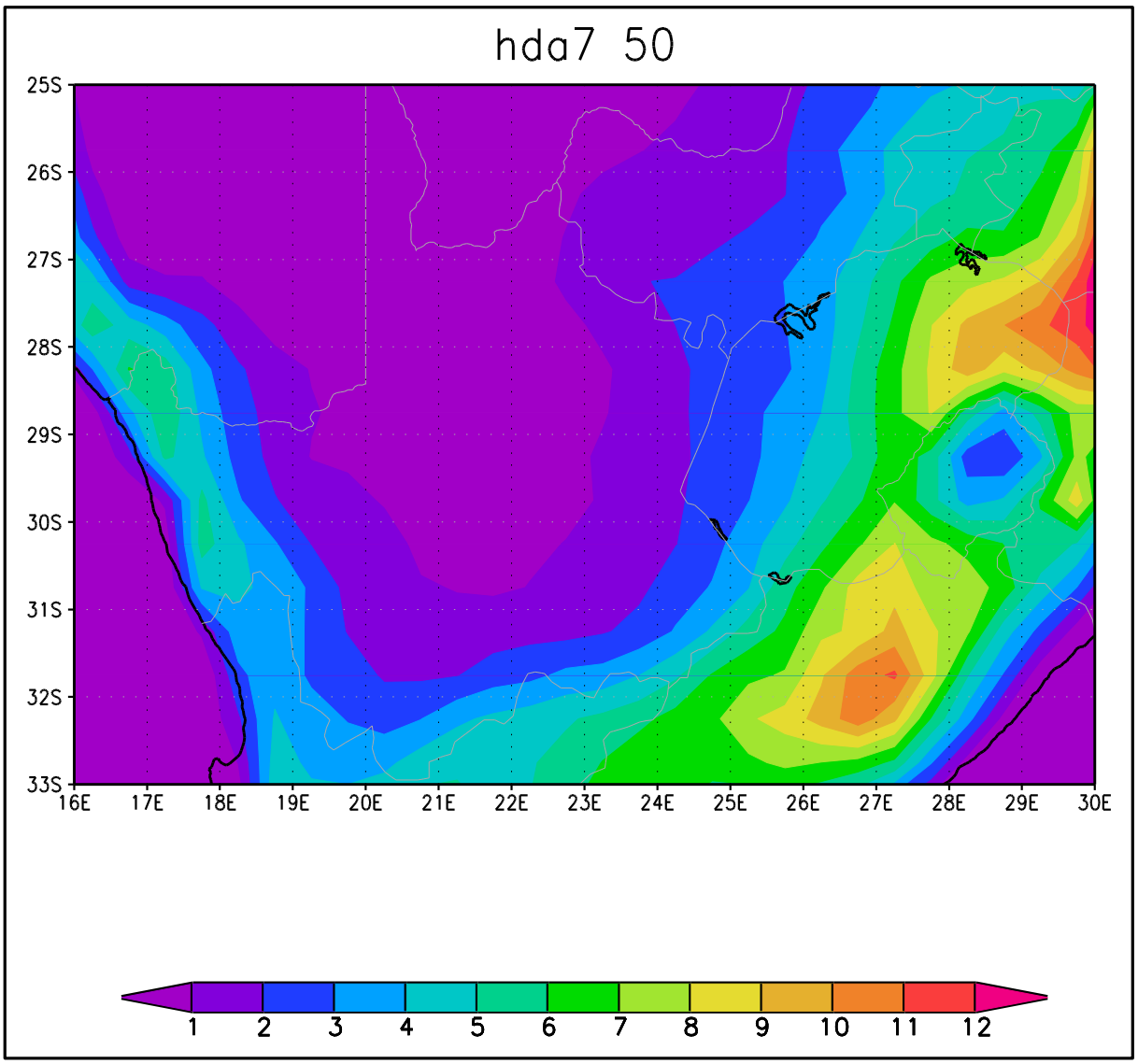


Figure 3.3 a: CCAM simulated annual average number of heat-wave days (units are number of days per grid point per year) over the Northern Cape, for the baseline period 1971-2000. The median of simulations is shown for the ensemble of downscalings of six GCM simulations.

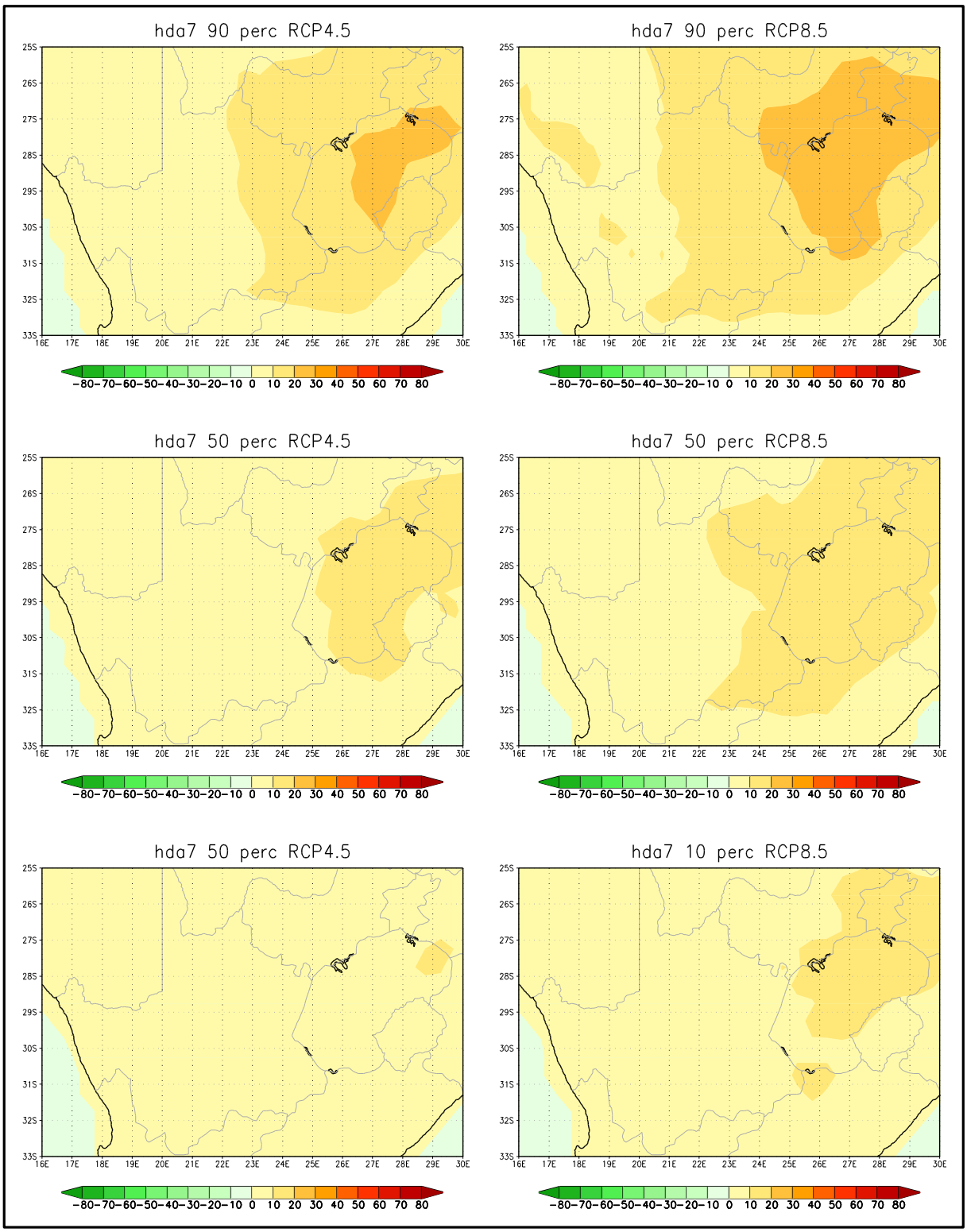
hda7 90 perc RCP4.5
hda7 90 perc RCP8.5
hda7 50 perc RCP4.5
hda7 50 perc RCP8.5
hda7 50 perc RCP4.5
hda7 10 perc RCP8.5
25S 26S 27S 28S 29S 30S 31S 32S 33S
16E 17E 18E 19E 20E 21E 22E 23E 24E 25E 26E 27E 28E 29E 30E
−80 −70 −60 −50 −40 −30 −20 −10 0 10 20 30 40 50 60 70 80

Figure 3.3 b (a-f): CCAM projected change in the annual average number of heat-wave days (units are number of days per grid point per year) over the Northern Cape for the time-slab 2020-2050 relative to 1971-2000. The 10th, 50th and 90th percentiles are shown for the ensemble of downscalings of six GCM projections under RCP4.5 (let) and RCP8.5 (right).

### 3.2.4 High fire danger days

Under present-day climate the largest numbers of high fire-danger days are projected to occur over the northern parts of the province (Figure 3.4 a), where the burning potential is low in the arid and semi-arid landscapes.

- In association with the drastic increase in temperatures and heat waves in the area, the high fire danger days are also expected to increase significantly over the Northern Cape.
- Under low mitigation the period 2020-2050 is projected to experience an increase in the number of high fire danger days. The increase is projected to be between 30 and 60 days per year in the north eastern parts of the province, where the burning potential is also the highest.
- Under the high mitigation scenario the increase in the number of high fire danger days is expected to range between 10 and 60 (Figure 3.4 b (a-f)).

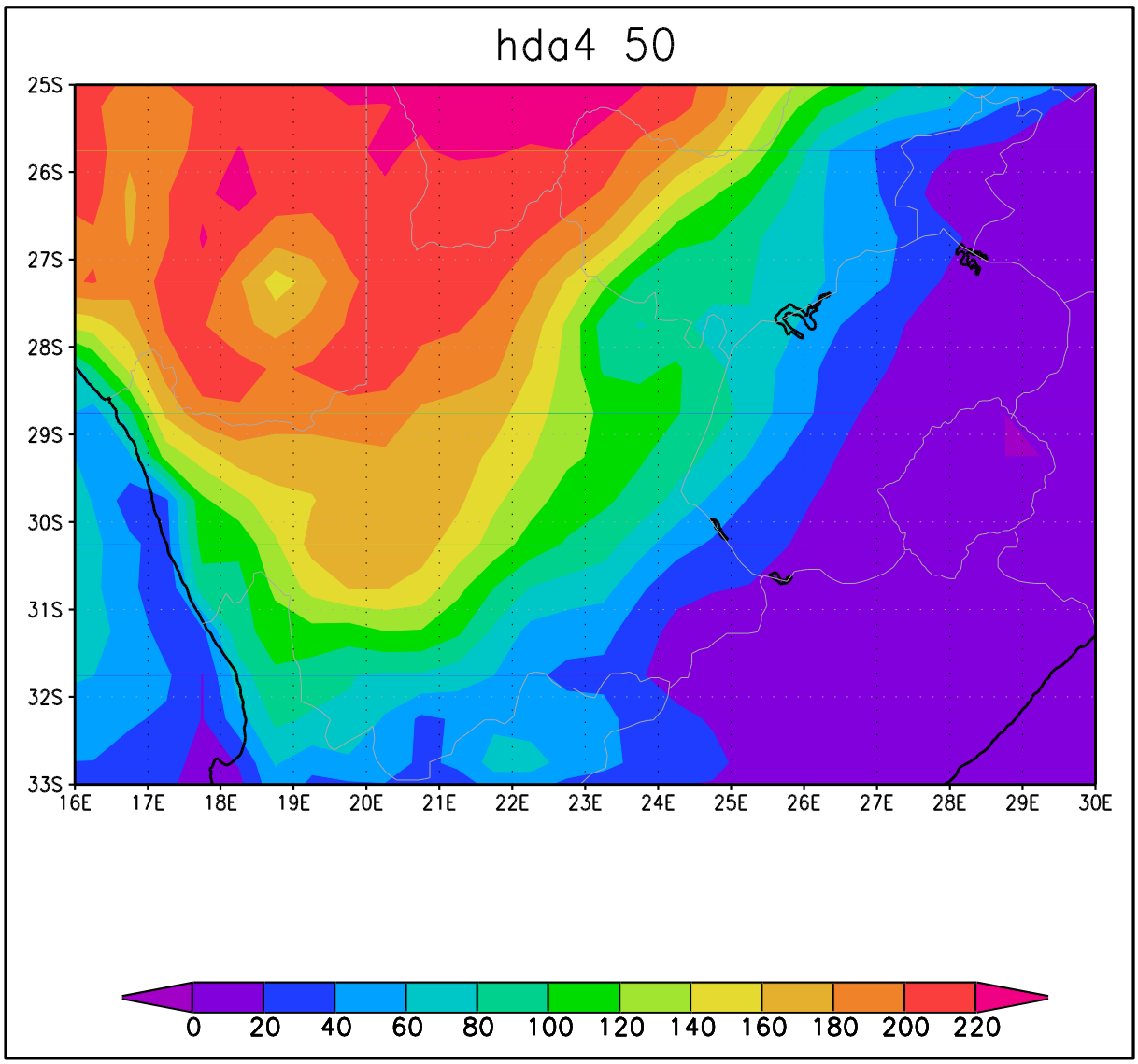


Figure 3.4 a: CCAM simulated annual average number of high fire-danger days (units are number of days per grid point per year) over the Northern Cape for the baseline period 1971-2000. The median of simulations is shown for the ensemble of downscalings of six GCM simulations.

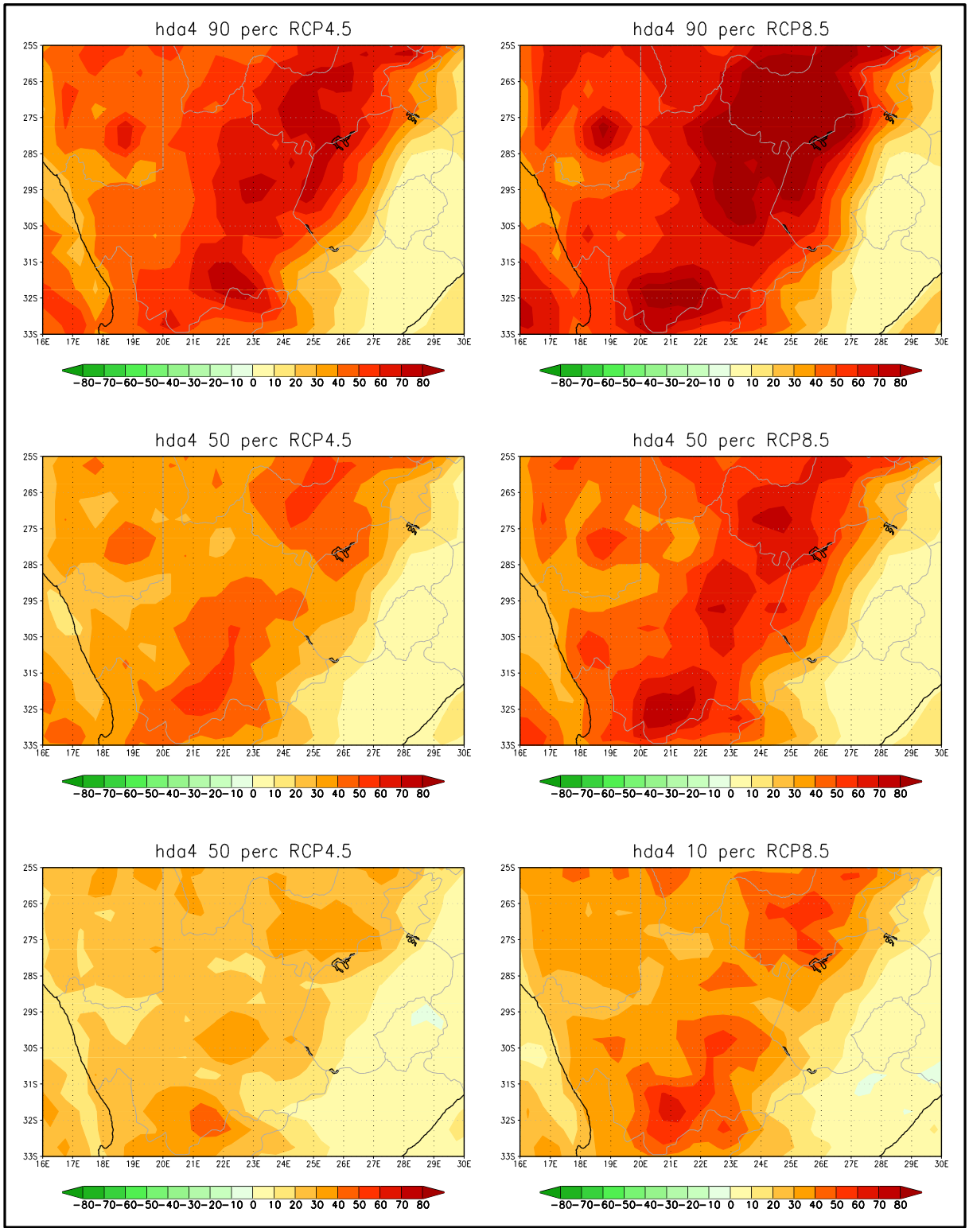
hda4 90 perc RCP4.5
hda4 90 perc RCP8.5
hda4 50 perc RCP4.5
hda4 50 perc RCP8.5
hda4 50 perc RCP4.5
hda4 10 perc RCP8.5
25S 26S 27S 28S 29S 30S 31S 32S 33S
16E 17E 18E 19E 20E 21E 22E 23E 24E 25E 26E 27E 28E 29E 30E
-80 -70 -60 -50 -40 -30 -20 -10 0 10 20 30 40 50 60 70 80

Figure 3.4 b (a-f): CCAM projected change in the annual average number of high fire-danger days (units are number of days per grid point per year) over the Northern Cape for the time-slab 2021-2050 relative to 1971-2000. The 10th, 50th and 90th percentile are shown for the ensemble of downscalings of six GCM projections under RCP4.5 (left) and RCP8.5 (right).

### 3.2.5 Average Rainfall

The Northern Cape is classified as an arid to semi-arid region, with annual rainfall totals being less than 500 mm over the eastern parts of the province, decreasing further towards the west (Figure 3.5 a ).

- General decreases in rainfall are projected for the Northern Cape under both high and low mitigation, by most ensemble members, for the period 2020-2050, relative to the present day condition. However, most ensemble members project rainfall increases over the north eastern parts of the province (Figure 3.5 a a-f)).
- Policy makers are advised to plan for the possibilities of both wetter and drier conditions over the eastern parts of the province, since climate model projections are indicative of both these regional features being plausible.

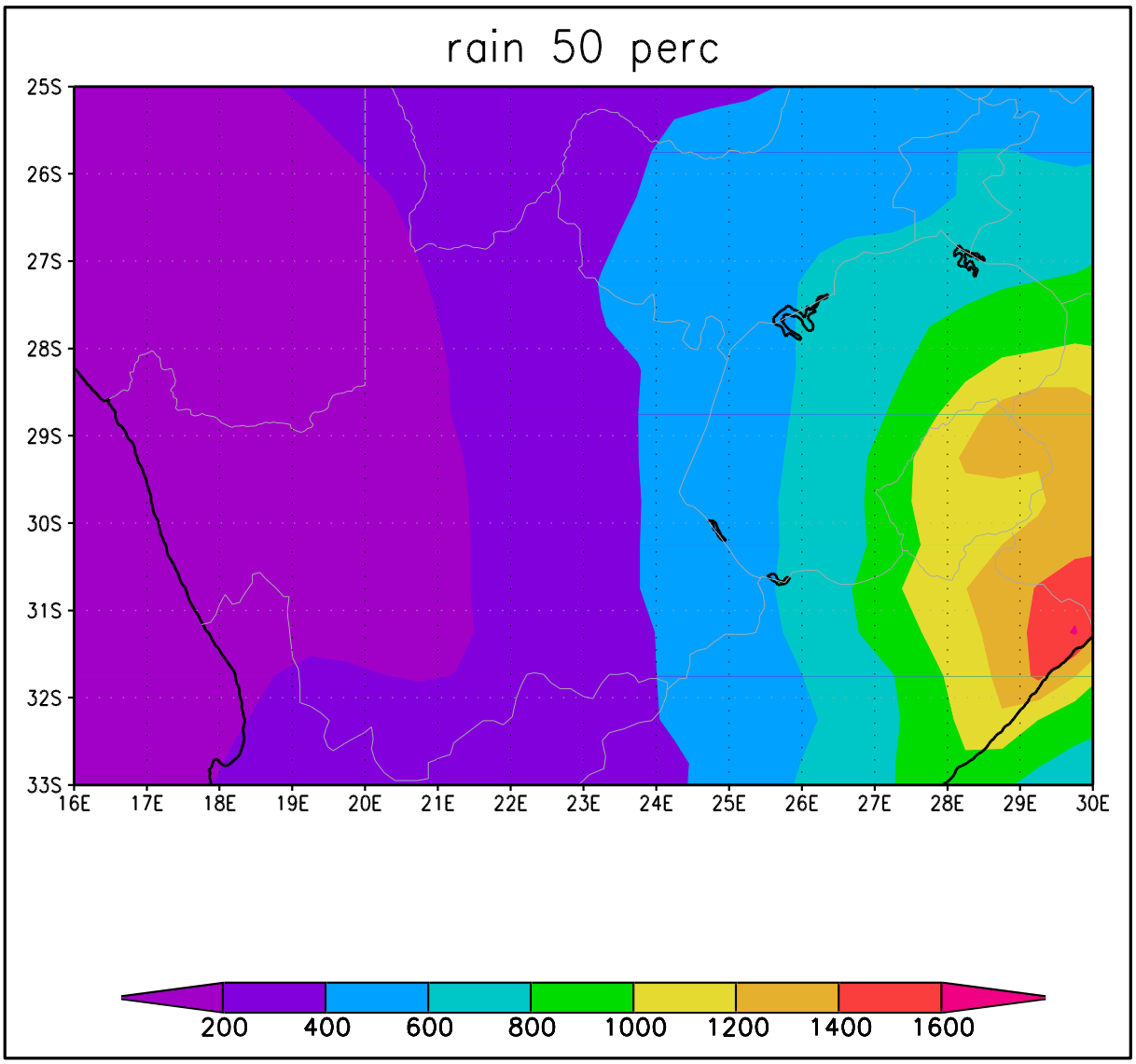


Figure 3.5 a: CCAM simulated annual average rainfall totals (mm) over the Northern Cape for the baseline period 1971-2000. The median of simulations is shown for the ensemble of downscalings of six GCM simulations.

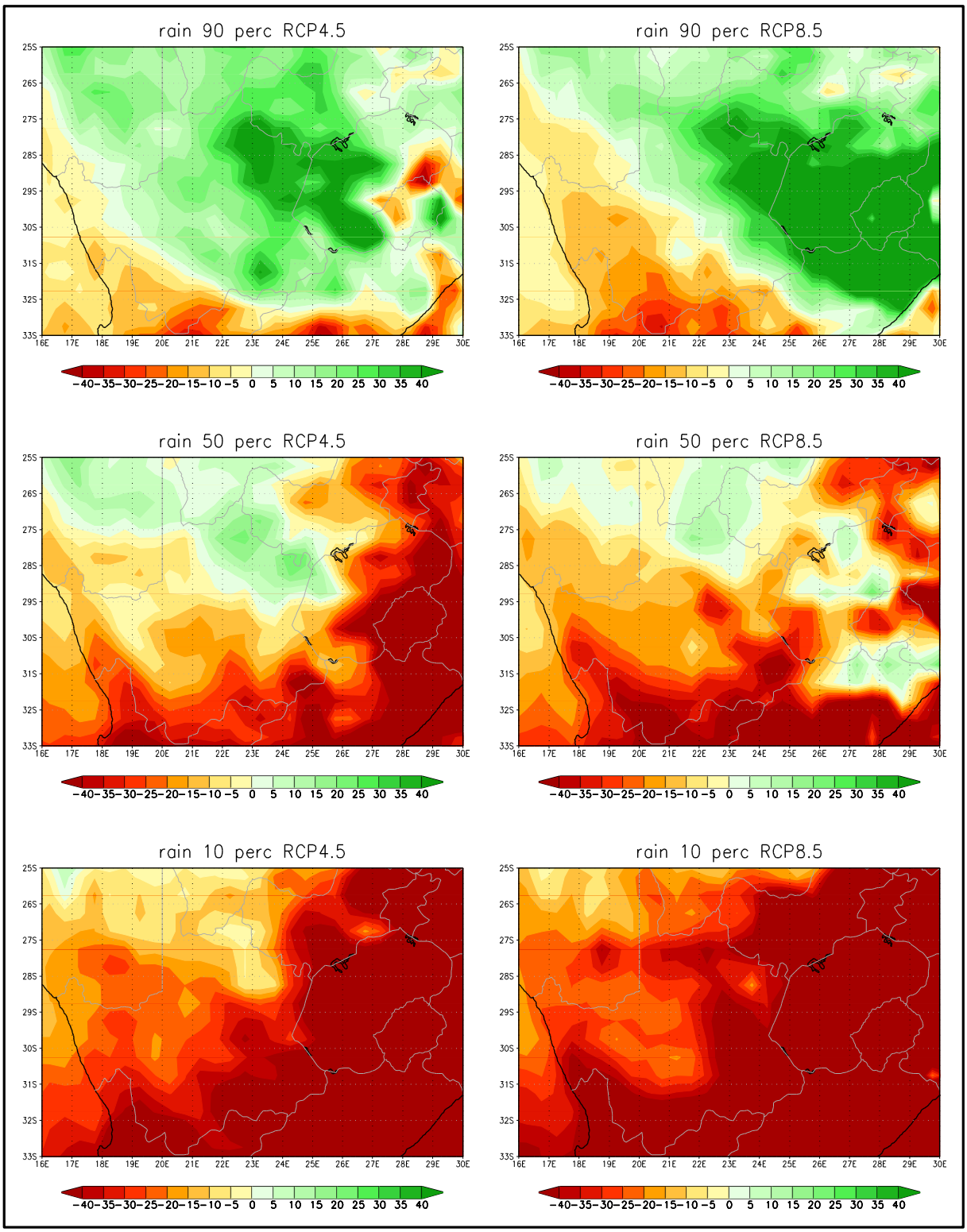
rain 90 perc RCP4.5
rain 90 perc RCP8.5
rain 50 perc RCP4.5
rain 50 perc RCP8.5
rain 10 perc RCP4.5
rain 10 perc RCP8.5
25S 26S 27S 28S 29S 30S 31S 32S 33S
16E 17E 18E 19E 20E 21E 22E 23E 24E 25E 26E 27E 28E 29E 30E
-40 -35 -30 -25 -20 -15 -10 -5 0 5 10 15 20 25 30 35 40

Figure 3.5 b (a-f): CCAM projected change in the annual average rainfall totals (mm) over central South Africa, covering Northern Cape for the time-slab 2020-2050 relative to 1971-2000. The 10$^{th}$, 50$^{th}$ and 90$^{th}$ percentiles are shown for the ensemble of downscalings of six GCM projections under RCP4.5 (left) and RCP8.5 (right).

### 3.2.6 Extreme rainfall events (including severe thunderstorms and lightning)

For the baseline period (1979-2000) the Northern Cape Province is simulated to experience only 2-4 extreme rainfall events per year at most locations ( Figure 3.6 a). The eastern part of the province is wetter and locations there are simulated to experience 3-4 extreme rainfall events per year.

- For the 2020-2050 period relative to the present day conditions the Northern Cape is projected to experience a decrease in number of extreme rainfall events by most ensemble members. Such decline is projected for both low and high mitigation futures.
- A minority of downscalings is indicative of an increase in extreme rainfall events over the northern parts of the province (Figure 3.6 b (a-f)).

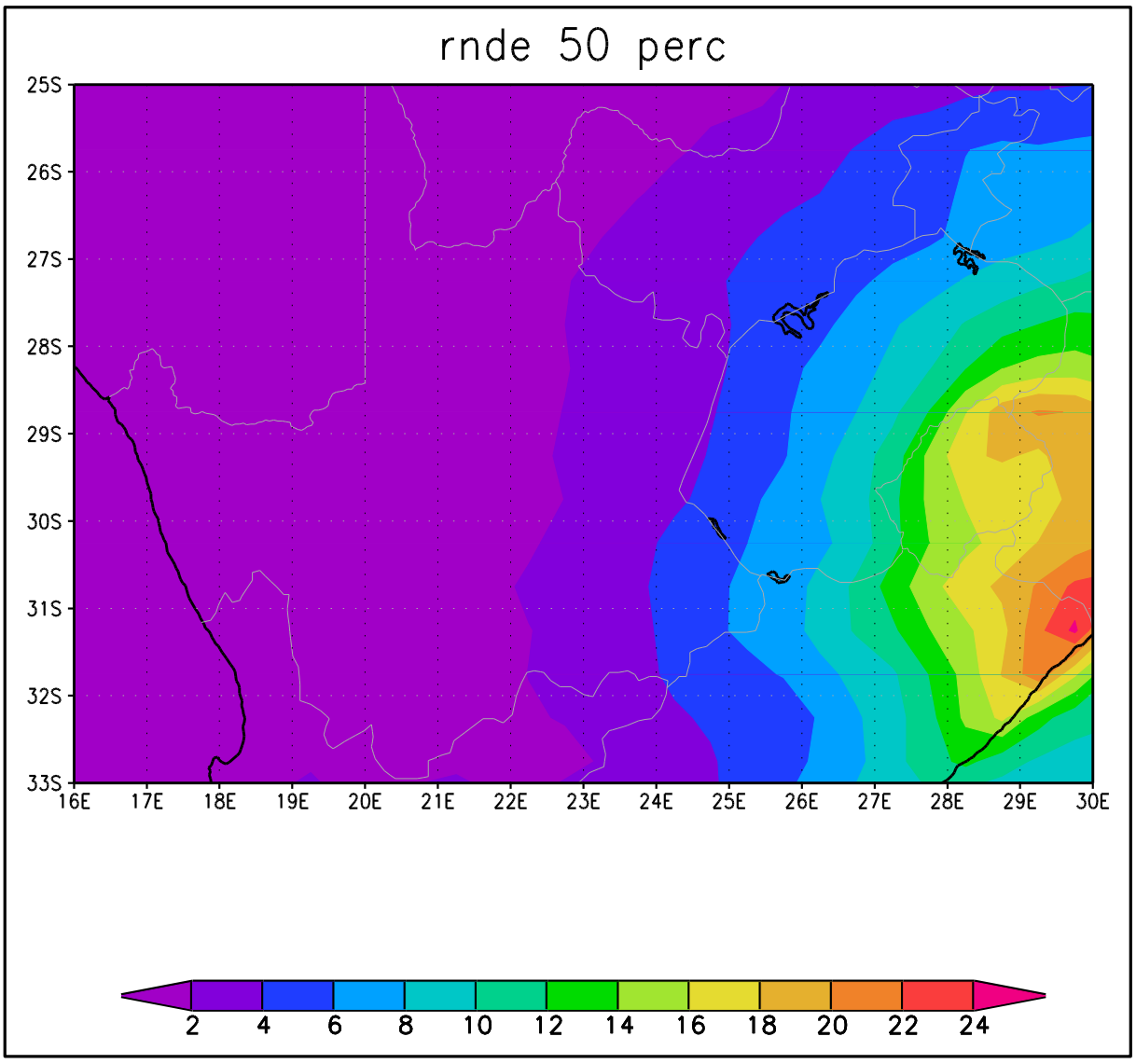


Figure 3.6 a: CCAM simulated annual average number of extreme rainfall days (units are number of days per grid point per year) over the Northern Cape for the baseline period 1971-2000. The median of simulations is shown for the ensemble of downscalings of six GCM simulations.

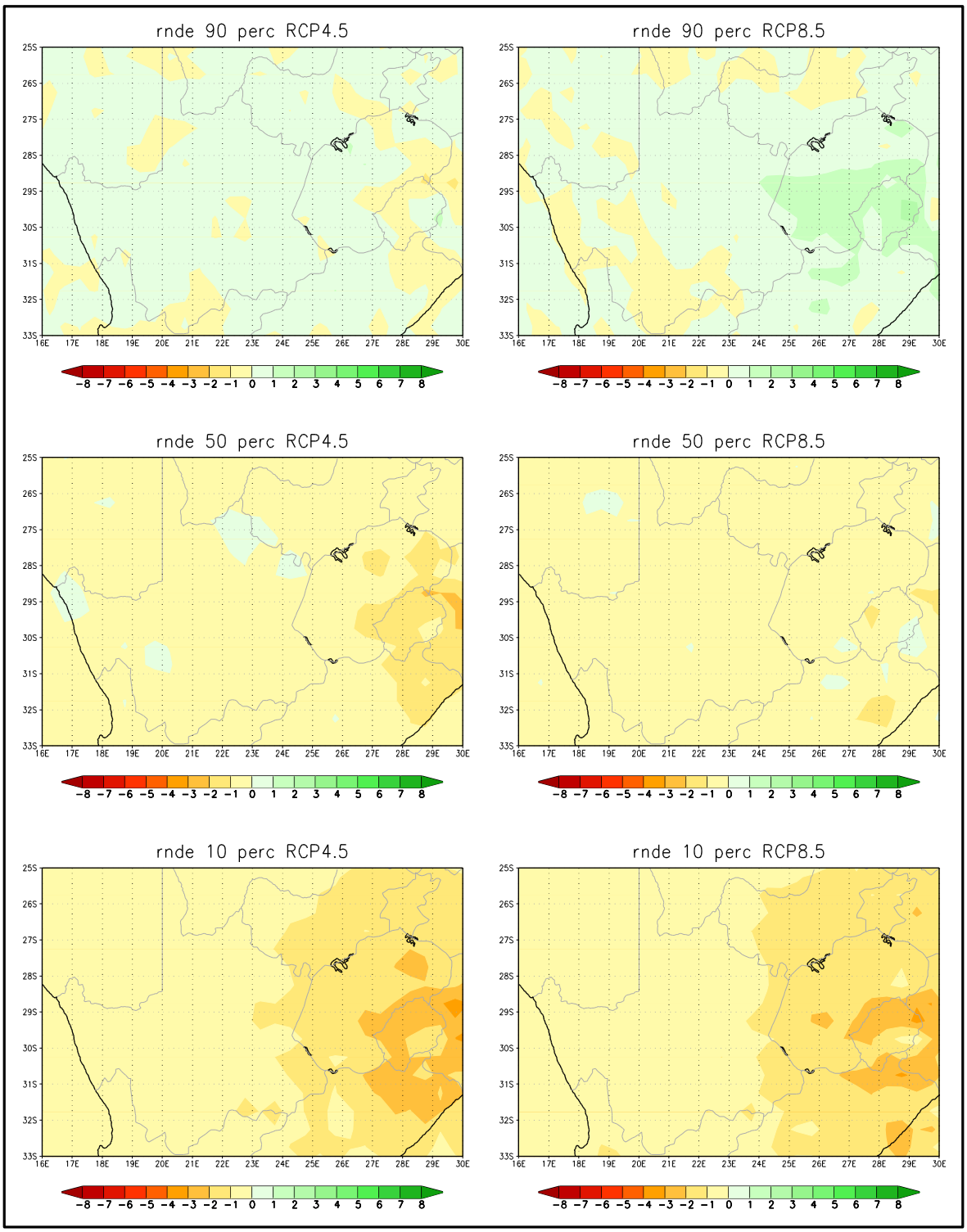


Figure 3.6 b (a-f): CCAM projected change in the annual average number of extreme rainfall days (units are numbers of grid points per year) over central South Africa, covering Northern

Cape for the time-slab 2020-2050 relative to 1971-2000. The 10th, 50th and 90th percentiles are shown for the ensemble of downscalings of six GCM projections under RCP8.5.

### 3.2.7 Dry spell days

For the present day conditions the model downscalings indicate that the province experiences between 100- 180 dry spell days per average. The number of dry spell days increases northwards towards Namibia (Figure 3.7 a).

- A robust pattern of increasing numbers of dry spell days is shown by the model downscalings (Figure 3.7 b (a-f)) for both high and low mitigation futures.

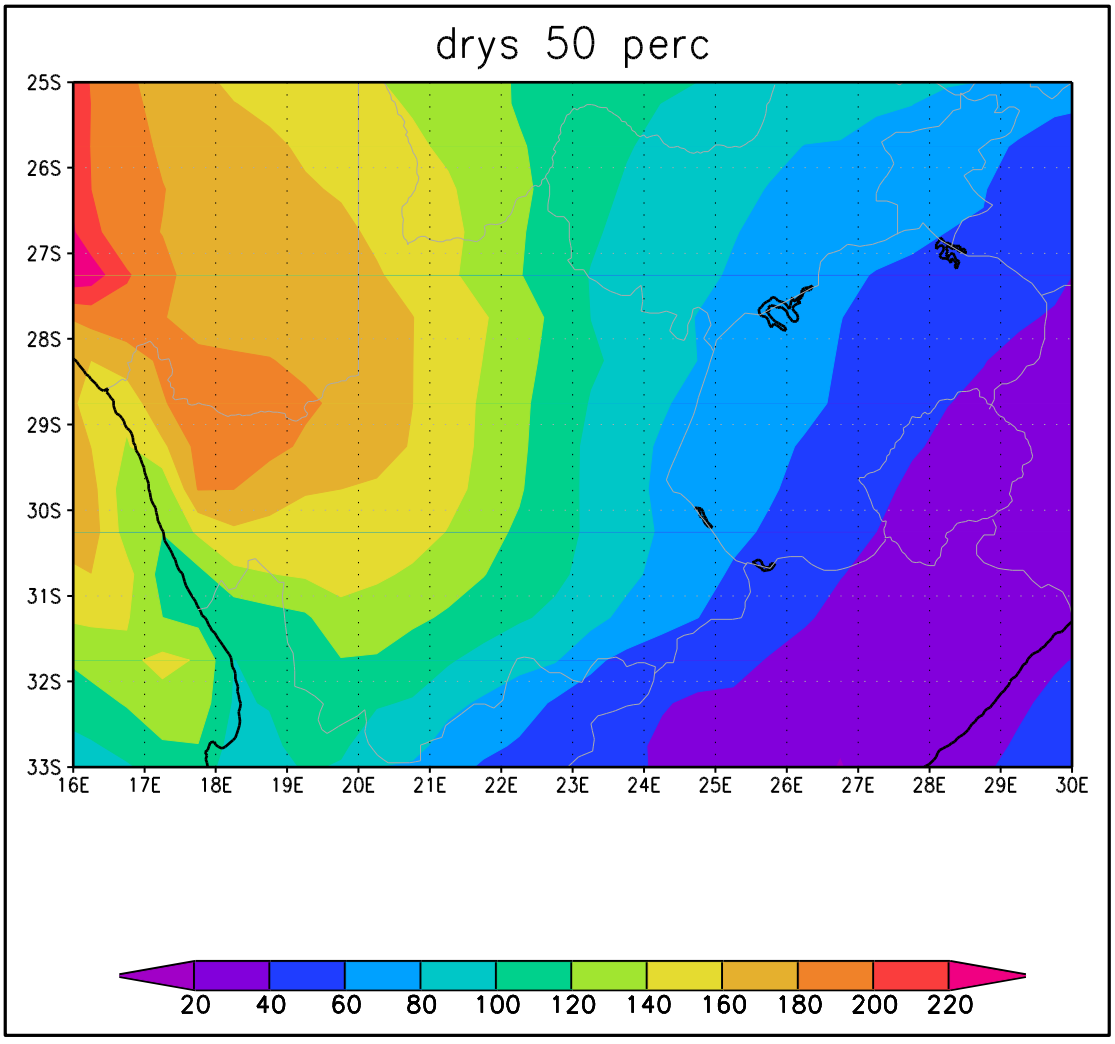


Figure 3.7 a: CCAM simulated annual average number of dry-spell days (units are number of days per grid point per year) over central South Africa, covering Northern Cape for the baseline period 1971-2000. The median of simulations is shown for the ensemble of downscalings of six GCM simulations.

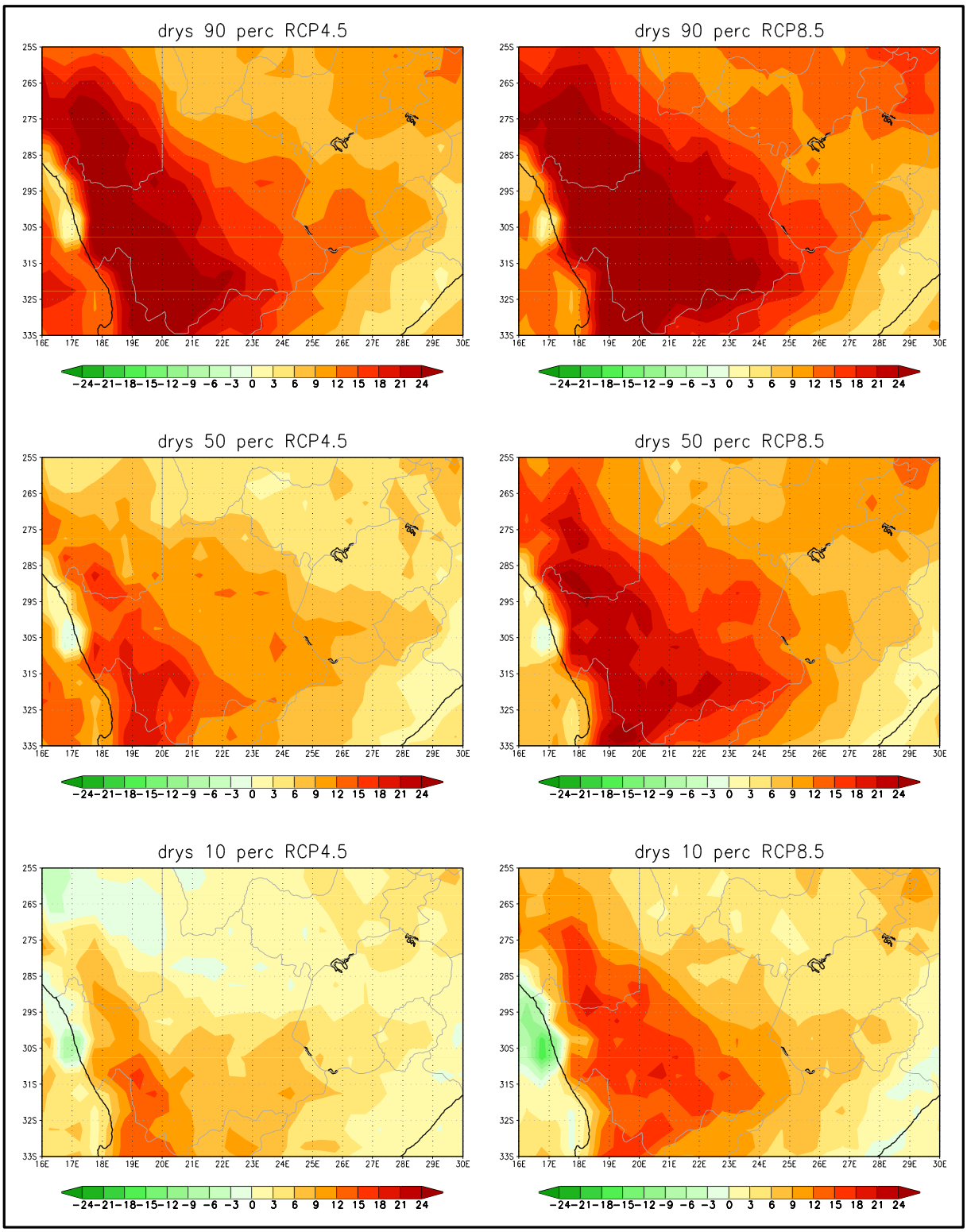
drys 90 perc RCP4.5
drys 90 perc RCP8.5
drys 50 perc RCP4.5
drys 50 perc RCP8.5
drys 10 perc RCP4.5
drys 10 perc RCP8.5
25S 26S 27S 28S 29S 30S 31S 32S 33S
16E 17E 18E 19E 20E 21E 22E 23E 24E 25E 26E 27E 28E 29E 30E
-24 -21 -18 -15 -12 -9 -6 -3 0 3 6 9 12 15 18 21 24

Figure 3.7 b (a-f): CCAM projected change in the annual average number of dry-spell days (units are numbers of grid points per year) over South Africa, covering the Northern Cape for the time-slab 2021-2050 relative to 1971-2000. The 10$^{th}$, 50$^{th}$ and 90$^{th}$ percentiles are shown for the ensemble of downscalings of six GCM projections under RCP4.5 (left) and RCP8.5 (right).

# 4. Conclusion

This report is based on an ensemble of high-resolution projections of future climate change over Africa, obtained by using the regional climate model CCAM to downscale the output of a number of CMIP5 (AR5) GCMs over Africa. The projections downscaled represent both high (RCP4.5) and low (RCP8.5) mitigation scenarios. CCAM was applied at 50 km resolution globally, and the experimental design of the simulations is consistent with that of CORDEX. The projections obtained are interpreted within the context of the GCM projections described in AR4 and AR5 of the IPCC and the regional projections of LTAS of DEA. The projected changes are presented for the period 2021-2050 relative to the 1971-2000 baseline period.

Under low mitigation, temperatures are projected to rise drastically, by 1-3 °C over the central South African interior for the period 2020-2050 relative to the baseline period. These increases are to be associated with increases in the number of very hot days, heat-wave days and high fire-danger days over South Africa. Key implications of these changes for NC province may include an increased risk for veld fires to occur in the grasslands areas. The household demand for energy in summer is also plausible to increase, to satisfy an increased cooling need towards achieving human comfort within buildings. Under high mitigation, the amplitudes of the projected changes in temperature and extreme temperature events are somewhat less, but still significant. The projected changes in rainfall and related extreme events exhibit more uncertainty than the projected temperature changes. A robust signal of increases in dry-spell-day frequencies is evident from the projections.

## 5. References


Christensen JH, Hewitson B, Busuioc A, Chen A, Gao X, Held I, Jones R, Kolli RK, Kwon W-T, Laprise R, Magana Rueda V, Mearns L, Menendez CG, Raisanen J, Rinke A, Sarr A, Whetton P (2007). *Regional climate projections.* In: Solomon S, Qin D, Manning M, Chen Z, Marquis M, Averyt, AB, Tignor M, Miller HL (eds). Climate change 2007: the physical science basis. Contribution of Working Group I to the Fourth Assessment Report of the Inter-governmental Panel on Climate Change. Cambridge University Press, Cambridge.

Engelbrecht CJ, Engelbrecht FA and Dyson LL (2013). High-resolution model projected changes in mid-tropospheric closed-lows and extreme rainfall events over southern Africa. *Int J Climatol* **33** 173–187. doi:10.1002/joc.3420.

Engelbrecht F, Adegoke J, Bopape MM, Naidoo M, Garland R, Thatcher M, McGregor J, Katzfey J, Werner M, Ichoku C and Gatebe C (2015). Projections of rapidly rising surface temperatures over Africa under low mitigation. *Environmental Research Letters. Submitted.*

Engelbrecht FA, Landman WA, Engelbrecht CJ, Landman S, Bopape MM, Roux B, McGregor JL and Thatcher M (2011). Multi-scale climate modelling over Southern Africa using a variable-resolution global model. *Water SA* **37** 647–658.

Engelbrecht FA, McGregor JL and Engelbrecht CJ (2009). Dynamics of the conformal-cubic atmospheric model projected climate-change signal over southern Africa. *Int J Climatol* **29** 1013–1033.

James R and Washington R (2013). Changes in African temperature and precipitation associated with degrees of global warming. *Climatic Change* **117** 859–872. DOI 10.1007/s10584-012-0581-7.

Katzfey KK, McGregor JM, Nguyen K and Thatcher M (2009). Dynamical downscaling techniques: Impacts on regional climate change signals. 18th World IMACS/MODSIM Congress, Cairns, Australia, July 2009.

Katzfey et al. (2012). High-resolution climate projections for Vietnam.

Kowalczyk EA, Garratt JR and Krummel PB (1994). Implementation of a soil-canopy scheme into the CSIRO GCM -regional aspects of the model response. CSIRO Div. Atmospheric Research Tech. Paper No. 32. 59 pp

LTAS (2013). Climate trends and scenarios for South Africa. Long-term Adaptation Scenarios Flagship Research Programme (LTAS). Phase 1, Technical Report no 6, pp 1-37. Contributors Midgley G., Engelbrecht F.A., Hewitson B., Chris J., New M., Tadross M., Schlosser A. and Dr Kenneth Strzepek.

Malherbe J, Engelbrecht FA and Landman WA (2013). Projected changes in tropical cyclone climatology and landfall in the Southwest Indian Ocean region under enhanced anthropogenic forcing. *Clim Dyn* **40** 2867–2886.

McGregor JL (2003). A new convection scheme using a simple closure. In: Current Issues in the Parameterization of Convection. BMRC Research Report 93. 33-36.

McGregor JL (2005). C-CAM: Geometric aspects and dynamical formulation. CSIRO Atmospheric Research Tech. Paper No 70, 43 pp.

McGregor JL and Dix MR (2001). The CSIRO conformal-cubic atmospheric GCM. In: Hodnett PF (ed.) Proc. IUTAM Symposium on Advances in Mathematical Modelling of Atmosphere and Ocean Dynamics. Kluwer, Dordrecht. 197-202.

McGregor JL and Dix MR (2008). An updated description of the Conformal-Cubic Atmospheric Model. In: Hamilton K and Ohfuchi W (eds.) High Resolution Simulation of the Atmosphere and Ocean. Springer Verlag. 51-76.

McGregor JL, Gordon HB, Watterson IG, Dix MR and Rotstayn LD (1993). The CSIRO 9-level atmospheric general circulation model. CSIRO Div. Atmospheric Research Tech. Paper No. 26. 89 pp

Mitchell TD and Jones PD 2005 An improved method of constructing a database of monthly climate observations and associated high-resolution grids. *International Journal of Climatology* **25** 693–712 DOI: 10.1002/joc.1181.

Niang I, Ruppel OC, Abdrabo M, Essel A, Lennard C, Padgham J, Urquhart P, Adelekan I, Archibald S, Barkhordarian A, Battersby J, Balinga M, Bilir E, Burke M, Chahed M, Chatterjee M, Chidiezie CT, Descheemaeker K, Djoudi H, Ebi KL, Fall PD, Fuentes R, Garland R, Gaye F, Hilmi K, Gbobaniyi E, Gonzalez P, Harvey B, Hayden M, Hemp A, Jobbins G, Johnson J, Lobell D, Locatelli B, Ludi E, Otto Naess L, Ndebele-Murisa MR, Ndiaye A, Newsham A, Njai S, Nkem, Olwoch JM, Pauw P, Pramova E, Rakotondrafara M-L, Raleigh C, Roberts D, Roncoli C, Sarr AT, Schleyer MH, Schulte-Uebbing L, Schulze R, Seid H, Shackleton S, Shongwe M, Stone D, Thomas D, Ugochukwu O, Victor D, Vincent K, Warner K, Yaffa S (2014). *IPCC WGII AR5* Chapter 22 pp 1-115.

Rotstayn LD (1997). A physically based scheme for the treatment of stratiform clouds and precipitation in large-scale models. I: Description and evaluation of the microphysical processes. *Quart. J. R. Meteorol. Soc.* **123** 1227-1282.

Schmidt F (1977). Variable fine mesh in spectral global model. Beitr. Phys. Atmos. **50** 211-217.

Schwarzkopf MD and Fels SB (1991). The simplified exchange method revisited: an accurate, rapid method for computation of infrared cooling rates and fluxes. *J. Geophys. Res.* **96** 9075-9096.

Thatcher M and McGregor JL (2009). Using a scale-selective filter for dynamical downscaling with the conformal cubic atmospheric model. *Mon. Weather Rev.* **137** 1742-1752

Thatcher M and McGregor JL (2010). A technique for dynamically downscaling daily-averaged GCM datasets over Australia using the Conformal Cubic Atmospheric Model. *Mon. Weather Rev.* **139** 79-95

Winsemius HC, Dutra E, Engelbrecht FA, Archer Van Garderen E, Wetterhall F, Pappenberger F and Werner MGF 2(014). The potential value of seasonal forecasts in a changing climate in southern Africa. *Hydrol. Earth Syst. Sci.* **18** 1525–1538.